Broadband Polarimetry with Radio Synthesis Arrays

W. D. Cotton (NRAO), June 21, 2023

***Abstract*—This memo describes tests using the Obit package of various options for doing broadband spectral imaging; in particular the imaging spectral resolution in Stokes Q and U and doing a joint Q/U deconvolution are considered. The trade-offs between spectral resolution and depth of CLEAN deconvolution that depend on the needed range of Faraday depth are explored. Also compared are an analysis of Q and U cubes using a direct search of Faraday depth and a least squares fitting of the peak Faraday depth and the EVPA at zero wavelength. Both work well in high signal-to-noise cases whereas in lower signal-to-noise cases the Faraday depth search remains robust while least squares fitting can give wild results.**

***Index Terms*—Polarimetry, Interoferometric Synthesis**

I. Introduction

RADIO sources that emit via the synchrotron process produce partially polarized radiation. In the optically thin case, the polarization angle of this emission gives the orientation on the sky of the magnetic field producing the synchrotron radiation.

Furthermore, any magnetized thermal plasma along the line of sight between the emission and observer will rotate the orientation of the polarization ("Faraday rotation"). A linearly polarized wave passing through a magnetized plasma will experience a Faraday rotation [1]:

$$\Delta\chi \;=\; \lambda^2\; 0.81 \int n_e B_{\|} dr, \tag{1}$$

where λ is the wavelength in m, n_e is the electron density in cm^{-3}, $B_{\|}$is the strength of the component of the magnetic field along the line of sight in μGauss and r is distance in parsec. This effect is commonly used to detect and quantify such intervening material. The range of Faraday depths that can be probed depends on the spectral resolution in the Q and U image cubes projects.

Imaging of continuum radio interferometer data has traditionally been done a spectral channel at a time. With wide-band systems the sensitivity of the aggregate spectrum may vastly exceed that of a single channel and a wide-band deconvolution may become desirable. The constraints on imaging polarized intensity (Stokes Q, U or V) are similar to those for Stokes I so the implementation of Obit task MFImage described in [2] is appropriate. This program divides the spectrum into a number of spectral sub-band of equal fractional bandwidth which are imaged independently and CLEANed jointly. In MFImage the spectral resolution of the products produced is controlled by the parameter maxFBW (maximum fractional bandwidth) which determines the channelization used. Since the range of Faraday depths which can be recovered depends on the sampling in wavelength^2, hence frequency, finer spacing in frequency may be needed for Q and U than in I.

When regions of high Faraday depth are imaged with a wide-band system, the polarization angle (mix of Q and U) will have a significant rotation across the bandwidth. This can decorrelate the Q or U signals across the bandwidth, or, in more extreme cases, across individual subband channels. If the Q and U image/deconvolution is done separately, this may cause regions of high Faraday depth to be inadequately deconvolved. Side-lobes may be misinterpreted as polarized features.

Instead of deconvolutions driven by the band average Q or U, a joint Q/U deconvolution driven by the subband average polarized intensity ($\sqrt{(Q^2+U^2)}$) can be used. In MFImage this option is invoked using the parameter doQU=True. This allows deconvolution of even very large Faraday depth emission.

The cost of averaging the polarized intensity across many spectral subbands is that this incoherent averaging reduces the residual noise much more slowly than a coherent averaging. In the low signal-to-noise regime, the noise reduces more like the fourth root of the number of subbands rather than the square root for a coherent average. This can limit the depth of the CLEAN.

This memo describes polarization imaging techniques and trade-offs in task MFImage from the Obit package [3][1]. Examples using data from the MeerKAT array are described.

II. RM Depth and Spectral Resolution

The frequency dependence of Faraday rotation will cause a rotation of the polarization angle across individual subband channels. This reduces the amplitude of the channel emission. If this reduction is large enough, the feature(s) affected can be lost all together. The range of Faraday depths adequately sampled depends on the frequency coverage and channelization.

In order to probe this effect, data-sets were simulated using MeerKAT L band frequency coverage including gaps due to persistent, strong RFI. A range of Faraday depths was included. These simulated images were then processed by Obit task RMSyn [5] to determine the response at the simulated depth. The averaging effect in actual data was simulated calculating the polarized response on a frequency grid 10 times finer than the actual instrumental basic channelization and making subband averages.

Three sets of simulations were done using maxFBW = 0.05 (14 channels), 0.01 (68 channels) and 0.005 (223 channels). These are shown in Figure 1. These panels show the range

National Radio Astronomy Observatory, 520 Edgemont Rd., Charlottesville, VA, 22903 USA email: bcotton@nrao.edu

[1]http://www.cv.nrao.edu/∼bcotton/Obit.html

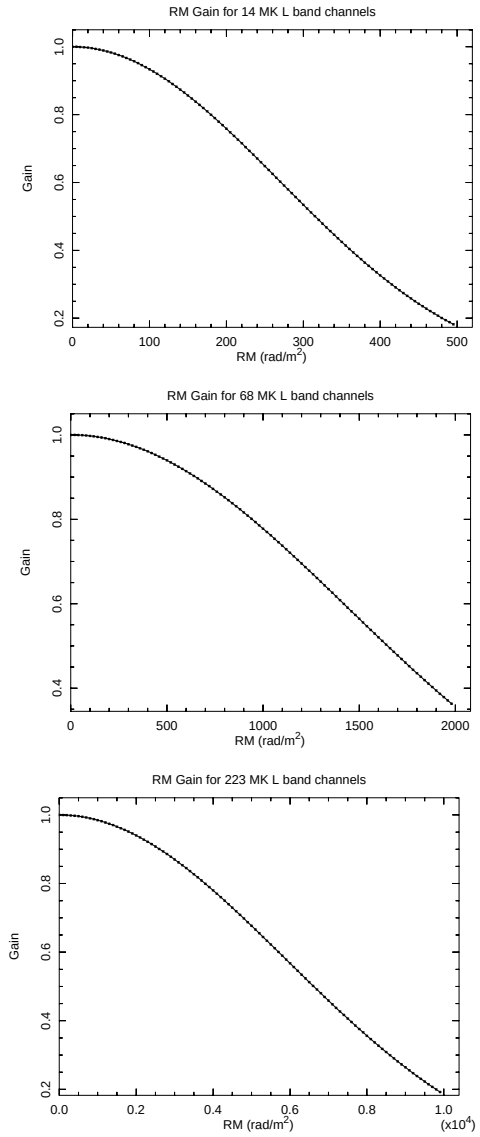

Fig. 1. Fraction of peak polarized intensity recovered as a function of Faraday depth for various spectral resolutions in MFImage.
top: maxFBW=0.05(14 channels)
middle:maxFBW=0.01 (68 channels)
bottom: maxFBW=0.005 (223 channels).

of Faraday depth that can be probed with each of these channelizations.

The half power range of Faraday depths for the different spectral resolutions is given in Table I. Many practical cases are covered with the lowest resolution tested; even moderate Faraday depth cases are covered in the intermediate case.

III. Average Polarized Intensity Noise

The increase in "noise" in the polarized intensity images used to drive the CLEAN deconvolution was explored using a full track MeerKAT L band data set (cluster of galaxies J0627.2-5428 [4], [5]). Average subband pixel polarized intensities were computed by script $OBIT/share/scripts/AvgMFPol.py. The pixel distributions from three different channelizations are shown in Figure 2.

TABLE I
50% Range of MeerKAT L band Spectral Resolutions

No. chan.	maxFBW	half power Faraday depth rad/m^2
14	0.05	$\pm$305
68	0.01	$\pm$1650
223	0.005	$\pm$6700

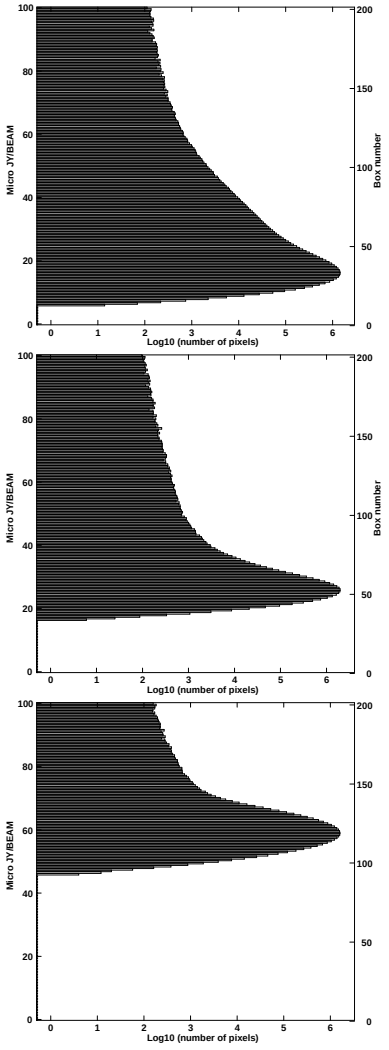

Fig. 2. Distribution of pixel average polarized intensity for a variety of imaging spectral resolutions in MFImage.
top: maxFBW=0.05 (14 channels)
middle:maxFBW=0.01 (68 channels)
bottom: maxFBW=0.005 (223 channels).

The difference between incoherent and coherent averaging is illustrated in Table II for the three spectral resolutions tested. Column "Peak Pol. Int." is the peak in the incoherent $\sqrt{(Q^2+U^2)}$ average distribution shown in Figure 2 and column "Q,U RMS" is the averge RMS of the coherent averages of the same Q and U cubes. The joint Q/U CLEAN

TABLE II
INCOHERENT AND COHERENT AVERAGING

No. chan.	Peak Pol. Int. μJy	Q,U RMS μJy
14	16.5	3.7
68	25.9	2.9
223	59.0	6.2

deconvolution driven by the polarized intensity will have the depth of the CLEAN limited by the greatly increased "noise" from the incoherent averaging.

IV. PEAK FINDING WITH FARADAY SYNTHESIS OR Q/U FITTING

There are two general techniques in wide use for analysing Q and U cubes to determine the dominant Rotation Measure, Electric Vector Polarization Angle (EVPA) and polarized intensity. These are a search in Faraday depth space for the RM which gives the largest, derotated polarized intensity and doing a nonlinear least squares fitting to Q+iU. These can both be used to estimate the peak Faraday depth and EVPA evaluated at zero wavelength but in the Obit implementations, only the former directly estimates the polarized intensity.

Obit python function RMFit.Cube has implementation of both these techniques controlled by the parameter doRMSyn. If doRMSyn is True, then the Faraday depth search is used else a least squares fitting. Since the least squares fitting is nonlinear, it needs an initial guess which is derived from a coarse search in Faraday depth. In the high signal-to-noise per subband channel regime, the least squares fitting works well and can also give estimates of the errors in the fitted parameters. In the low signal-to-noise regime, the Faraday depth search is more robust. Tests with simulated data were used to explore how the two techniques work in the intermediate signal-to-noise regime.

A simulation similar to that used for Section II was used with various levels of added noise. Thirty instances each of simulated data for Faraday depths of 50, 100 and 200 rad/m^2 using 68 channel spectral resolution were made. The resultant Q and U cubes were analysed using the two options in RMFit.Cube and the fits compared. The Faraday depth search results were fairly robust over the range of signal-to-noise tested but the least squares fitting sometimes converged to wild answers in the higher noise cases. To remove most of these wild fits, the 4 most discrepant comparisons in each of the groups of 30 trials were discarded. The comparisons are given in Figure 3. In the lower added noise cases, both techniques worked well but the scatter in the differences increased with increasing noise. The scatter in the RM and EVPA differences did not seem to be affected by the RM of the test source.

V. DISCUSSION

A combination of adequate Faraday depth coverage and depth of deconvolution of the polarized (Stokes Q,U) emission may be obtained with the appropriate values of the maximum fractional bandwidth (maxFBW) and joint Q/U deconvolution (doQU). Higher imaging spectral resolution is needed to recover large (absolute) values of Faraday depth. Large Faraday depths will reduce the sensitivity of band averaged Q or U images used to drive the CLEAN deconvolution causing regions of high Faraday depth to be less deconvolved. This effect can be reduced using a joint Q & U deconvolution driven by the subband average polarized intensity. The incoherent avaraging inherent in the joint deconvolution increases the effective noise and can also limit the depth of the deconvolution.

The spectral resolution needed is a compromise between the needed good sensitivity to a range of Faraday depth and the decrease in the depth of a possible CLEAN with increasing spectral resolution using a joint Q/U deconvolution. The requirements depend on the circumstances of the target source.

In the low noise (high signal to noise) regime both a Faraday depth search and a Q/U least squares fitting work well and give comparable results. At higher noise levels the least squares fitting occasionally gives wild results but the Faraday depth search remains robust.

REFERENCES

[1] M. A. Brentjens and A. de Bruyn, "Faraday rotation measure synthesis," *A&A*, vol. 441, pp. 1217–+, Sep. 2005.

[2] W. D. Cotton, J. J. Condon, K. I. Kellermann, M. Lacy, R. A. Perley, A. M. Matthews, T. Vernstrom, D. Scott, and J. V. Wall, ""The Angular Size Distribution of μjy Radio S"ources"," *ApJ*, vol. 856, p. 67, 2018.

[3] W. D. Cotton, "Obit: A Development Environment for Astronomical Algorithms," *PASP*, vol. 120, pp. 439–448, 2008.

[4] K. Knowles, W. D. Cotton, L. Rudnick, F. Camilo, S. Goedhart, R. Deane, M. Ramatsoku, M. F. Bietenholz, M. Brüggen, C. Button, H. Chen, J. O. Chibueze, T. E. Clarke, F. de Gasperin, R. Ianjamasimanana, G. I. G. Józsa, M. Hilton, K. C. Kesebonye, K. Kolokythas, R. C. Kraan-Korteweg, G. Lawrie, M. Lochner, S. I. Loubser, P. Marchegiani, N. Mhlahlo, K. Moodley, E. Murphy, B. Namumba, N. Oozeer, V. Parekh, D. S. Pillay, S. S. Passmoor, A. J. T. Ramaila, S. Ranchod, E. Retana-Montenegro, L. Sebokolodi, S. P. Sikhosana, O. Smirnov, K. Thorat, T. Venturi, T. D. Abbott, R. M. Adam, G. Adams, M. A. Aldera, E. F. Bauermeister, T. G. H. Bennett, W. A. Bode, D. H. Botha, A. G. Botha, L. R. S. Brederode, S. Buchner, J. P. Burger, T. Cheetham, D. I. L. de Villiers, M. A. Dikgale-Mahlakoana, L. J. du Toit, S. W. P. Esterhuyse, G. Fadana, B. L. Fanaroff, S. Fataar, A. R. Foley, D. J. Fourie, B. S. Frank, R. R. G. Gamatham, T. G. Gatsi, M. Geyer, M. Gouws, S. C. Gumede, I. Heywood, M. J. Hlakola, A. Hokwana, S. W. Hoosen, D. M. Horn, J. M. G. Horrell, B. V. Hugo, A. R. Isaacson, J. L. Jonas, J. D. B. Jordaan, A. F. Joubert, R. P. M. Julie, F. B. Kapp, V. A. Kasper, J. S. Kenyon, P. P. A. Kotzé, A. G. Kotze, N. Kriek, H. Kriel, V. K. Krishnan, T. W. Kusel, L. S. Legodi, R. Lehmensiek, D. Liebenberg, R. T. Lord, B. M. Lunsky, K. Madisa, L. G. Magnus, J. P. L. Main, A. Makhaba, S. Makhathini, J. A. Malan, J. R. Manley, S. J. Marais, M. D. J. Maree, A. Martens, T. Mauch, K. McAlpine, B. C. Merry, R. P. Millenaar, O. J. Mokone, T. E. Monama, M. C. Mphego, W. S. New, B. Ngcebetsha, K. J. Ngoasheng, M. T. Ockards, A. J. Otto, A. A. Patel, A. Peens-Hough, S. J. Perkins, N. M. Ramanujam, Z. R. Ramudzuli, S. M. Ratcliffe, R. Renil, A. Robyntjies, A. N. Rust, S. Salie, N. Sambu, C. T. G. Schollar, L. C. Schwardt, R. L. Schwartz, M. Serylak, R. Siebrits, S. K. Sirothia, M. Slabber, L. Sofeya, B. Taljaard, C. Tasse, A. J. Tiplady, O. Toruvanda, S. N. Twum, T. J. van Balla, A. van der Byl, C. van der Merwe, C. L. van Dyk, V. Van Tonder, R. Van Wyk, A. J. Venter, M. Venter, M. G. Welz, L. P. Williams, and B. Xaia, "The MeerKAT Galaxy Cluster Legacy Survey I. Survey Overview and Highlights," *arXiv e-prints*, p. arXiv:2111.05673, Nov. 2021.

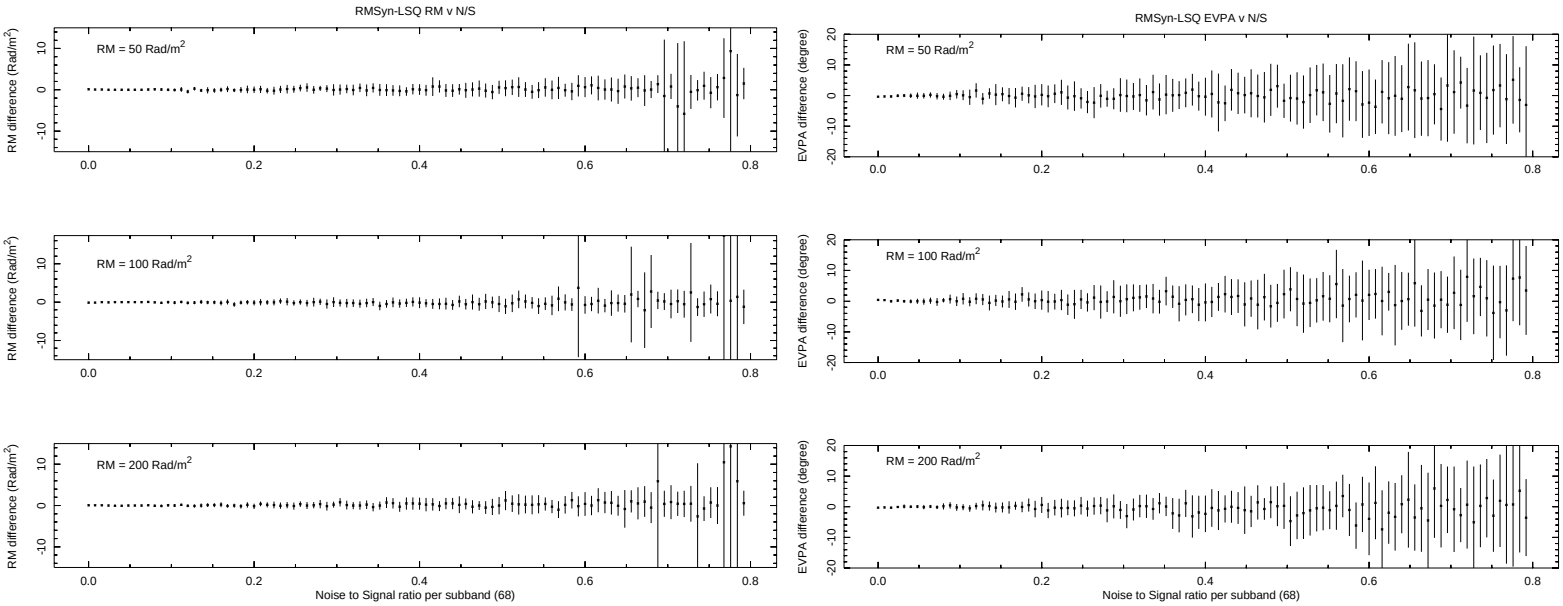

Fig. 3. Comparison of RM Synthesis and Q/U least squares fitting. Error bars show the RMS difference in multiple trials excluding the most discrepant 4 of 30 comparisons. 68 subband channel spectral resolution is used in this comparison.
Left: RM difference; the large RMS points are the result of failures in the least squares fitting.
Right: EVPA difference.

[5] L. Rudnick and W. D. Cotton, "Full resolution deconvolution of complex Faraday spectra," *MNRAS*, vol. 522, no. 1, pp. 1464–1479, Jun. 2023.